TWO PIECE JIG SAW PUZZLE ROBOT ASSEMBLY WITH VISION, POSITION AND FORCE FEEDBACK

Grigore C. Burdea[1]

Courant Institute of Mathematical Sciences
New York University
251 Mercer Street, New York, N.Y. 10012

ABSTRACT

This paper presents a robotic assembly of two 3-D jig-saw puzzle pieces, using vision, position and force feedback. Geometrical aspects are discussed together with force history of the experiments. An installation using 7565 I.B.M. robot with a CCD camera on the robot arm is described. Successful experiments proved the possibility of assembling parts with complex contours when force feedback is used during fine assembly.A videotape of the demonstration is available. RR 107/1987.

1.Introduction

Automated assembly of variable and complex shaped parts with relatively small tolerances is a substantially more demanding task than the peg in a hole problem treated in literature. Inoue[5], Simmunovic[10], Seltzer[9] have discussed force aspects of peg in a hole insertion, and demonstrated successful mating with small tolerances. Their approach was to consider the geometry of parts as known, and use complex force sensor to accommodate positioning errors during assembly. Further work by Lozano-Perez and Mason[7,8] developed automated synthesis fine motion strategies for peg in hole insertion. Buckley[2] extends automated synthesis to rectangular pegs in rectangular holes. In his motion synthesis Buckley simplifies the general problem by addressing translational errors only. The present work addresses aspects related to robot assembly of variable shaped parts such as jig-saw puzzles. Due to their complex geometry, rotational errors cannot be overlooked and are addressed during the fine assembly part of our implementation. We chose to use puzzle pieces since Kalvin, Schonberg and Wolfson[6], developed algorithms for simulated jig-saw puzzle assembly using vision.

[1] Associated with Department of Applied Science, New York University.

This paper describes techniques developed for automatic assembly of two puzzle pieces[3,4]. Future work will extend this results to robotic assembly of a whole jig-saw puzzle. Section 2 describes the experimental installation, sensor issues and puzzle piece modification for robot assembly. Section 3 presents vision to robot transformations for part detection and pick up, while Section 4 develops geometrical equations used during robot assembly. Robot moves are structured in *raw positioning,transition to fine assembly and fine assembly moves*. Section 5 presents force history and determines acceptable level of errors for successful assembly.

2. Experimental Installation

2.1 Description

The experimental system presented in Fig. 1 and 2 consists of an I.B.M. 7565 robot, vision system, force sensors and mechanical force amplifier. The vision system uses Fairchild CCD camera, with a 256x256 sensor array and a VICOM image processor. The Fairchild camera sensor head is installed directly on the robot arm,at fixed height above the robot work table. This eliminates the need for special lense drives.

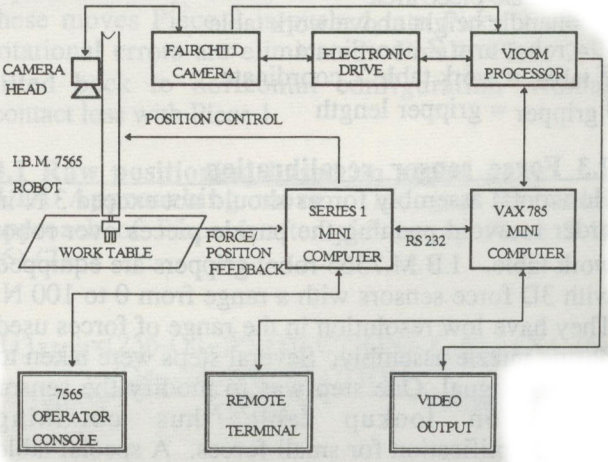

Fig. 1 Experimental installation

A VAX minicomputer supervises the vision process and communicates with a SERIES 1 robot controller. Force sensors on the robot gripper allow for force feedback during assembly. A combination of puzzle piece handle and specially designed gripper nails provides force amplification.

2.2 Piece Preparation

For our experiment we selected an "off the shelf" wooden puzzle and covered it with black non reflective paper. This was necessary in order to boost the quality of vision images. It is important to prevent slip on the work table during robot assembly. Therefore the bottom of the puzzle pieces was fitted with Koroseal flexible magnetic strip[1] that created a magnetic pull towards the metal work table. The magnitude of the magnetic force determines the assembly force envelope. These forces were determined experimentally to be about 1.4N/sq. inch or about 3 N for puzzle pieces with a surface of 2 to 3 sq. inches. The robot gripper configuration (2 parallel fingers) does not allow direct grasping of puzzle pieces. It was therefore necessary to mount a cylindrical handle on one of the puzzle pieces corresponding to its center of gravity. In this way the robot grasps on the handle when picking up the puzzle piece. Grasping has to be done without pushing or overturning. Maximum grasping force used in center grasp is given by (1).

$$F_{grasp} = \frac{2k_{mag}\ A\ l}{H + Z - l_{gripper} - Z_{table}} \quad (1)$$

F_{grasp} = maximum grasping force
l = distance from center of gravity to puzzle edge
h = grasping force application point versus table
k_{mag} = specific magnetic pulling force
A = puzzle piece area
H = handle height above work table
Z = robot arm Z coordinate
Z_{table} = work table Z coordinate
$l_{gripper}$ = gripper length

2.3 Force sensor recalibration

Horizontal assembly forces should not exceed 3 N in order to avoid pushing the puzzle pieces over robot work table. I.B.M.7565 robot grippers are equipped with 3D force sensors with a range from 0 to 100 N. They have low resolution in the range of forces used during puzzle assembly. Several steps were taken to amplify signal. One step was to modify the sensor calibration lookup table thus obtaining 100%amplification for small forces. A special table was created during a one time off-line calibration,

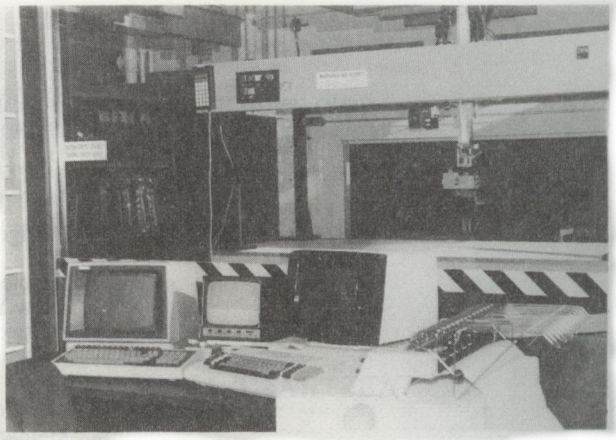

Fig. 2 IBM 7565 robot with vision system

and the low level software loaded in the system library. Since no high level software is involved, there was no impact on overall run time. The adverse result of this procedure was an increase in signal noise (or uncertainty) from 0.15 to 0.30 N. The other step to increase readings was to add specially designed gripper nails. These nails work as mechanical force amplifiers producing 50% pitch and side force amplification.

3. Vision steps for assembly

Vision steps are piece detection, feature extraction and visual match.

3.1 Camera coordinate transformations

For both visual search and piece pickup it is necessary to establish the correspondence between image and robot spaces. This relation is determined by a number of parameters such as *camera position offset* ,*camera x/y distortion factor* and *camera projection factor*. The camera position offset is the distance from the image center to x/y robot link in robot coordinates (Z coordinates are fixed and no rotation offset is taken into account). The x/y distortion factor is specific to each CCD camera and represents the number of pixels that corresponds to a given length along x and y axis. The projection factor depends on the lens used as well as camera to work table distance. It represents the number of inches per image pixel. Camera to robot coordinates transformation is expressed by (2),(3).

$$X_{rob}=(256-X_{vic})PROJECTION-X_{offset}+X \quad (2)$$

$$Y_{rob}=\frac{(Y_{vic}-240)PROJECTION}{XSCALE}-Y_{offset}+Y \quad (3)$$

X_{rob}, Y_{rob}= robot point coordinates
X_{vic}, Y_{vic}=VICOM point coordinates
Xoffset,Yoffset=camera offset
PROJECTION=projection factor
XSCALE=camera distortion factor
X,Y= robot arm coordinates

3.2 Work Table Visual Scan

As a matter of generality puzzle pieces are placed randomly on the work table, and their location is not known to the assembly algorithm. There are however limitations on the puzzle piece position which has to be within the intersection of camera field of view and robot work envelope. During initial assembly stage, we are interested to determine whether the puzzle pieces exist rather than extracting their shape. The visual scan therefore uses compressed images that give a significant processing speed up. Each image is analyzed to detect part presence and raw center of gravity. The vision system is a 2D system that takes images of a 3D scene. This produces vision errors if pieces are not centered under the camera. The robot has therefore the additional task of centering the camera on top of a discovered piece in order to minimize vision errors.

3.3 Shape extraction and visual match

Once the camera is centered on the puzzle piece, its shape is extracted using SHAPE and CORNER routines (Edith Schonberg). The output is a sampled curve divided into four sides as presented in Fig. 3. This becomes input for MATCH routine (A. Kalvin) that returns a score for matching sides of two puzzle pieces. Our algorithm selects the smallest of 16 match scores, corresponding to the two sides that most likely match. MATCH also returns the rotation and translation of the matching sides. Robot rotation and translation is done using the handle on the puzzle piece, rather than the matching sides. The target for the rotated puzzle piece is obtained from MATCH output using (4), (5).

$$G_{3x}=\frac{P2x+LEFTX(XSCALE-1)}{XSCALE}+ \quad (4)$$
$$+\sin(\theta)(G_{1y}-P_{1y})+\frac{\cos(\theta)(G_{1x}-P_{1x})}{XSCALE}$$

$$G3y=P2y+\frac{\sin(\theta)(P1x-G1x)}{XSCALE}+\cos(\theta)(G1y-P1y) \quad (5)$$

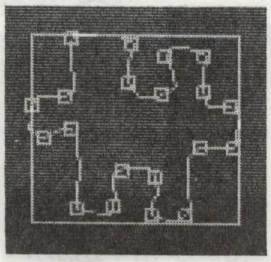

Fig. 3 CORNER output

$G_{3x,y}$ = center of gravity of rotating piece after rotation
$G_{1x,y}$ = center of gravity before rotation
$P_{1x,y}$ = center of gravity of matching side on rotating piece
$P_{2x,y}$ = center of gravity of matching side on stationary piece
θ= rotation angle of matching side (given by MATCH)
LEFTX = leftmost X_{vic} coordinate of stationary piece

4. Assembly steps

We have adopted Simmunovic's notation when considering the overall automated assembly as divided in three steps: raw positioning, transition to fine assembly and fine assembly. During *raw positioning* Piece 2 is picked up, rotated and translated to Piece 1, tilted and lowered on top of Piece 1. The raw positioning task is to bring Piece 2 in contact with Piece 1 in such a way as to allow further assembly moves to eliminate both rotation and translation errors. The strategy is to induce an overshoot of Piece 2 so that the relative position of the two pieces is disambiguated. During *transition moves* the two pieces remain in contact while their relative position changes to a nested configuration. and translational errors are eliminated. The final step is *fine assembly* based on force feedback. During these moves Piece 2 is pushed into Piece 1 while rotational errors are eliminated. Finally Piece 2 is tilted back to horizontal configuration without contact loss with Piece 1.

4.1 Raw positioning based on vision data

4.1.1 Approaching move The goal for initial approach of Piece 1 after picking up Piece 2 is (6),(7).

$$G_{3xrob}=(256-G_{3x})PROJECTION)-X_{offset}+X1 \quad (6)$$

$$G_{3yrob}=\frac{(G_{3y}-240)PROJECTION}{XSCALE}-Y_{offset}+Y1 \quad (7)$$

$G_{3x,y}$ =center of gravity of moving piece after rotation given by(4,5)
X_1, Y_1= robot arm coordinates when stationary piece was in center of image.
Z arm coordinates during this move are determined by collision avoidance criteria. Since no obstacles are present, this becomes a free space move.

4.1.2 Tilting move The piece that is picked up by robot has a convexity that has to get into the concavity of the stationary piece. Generally speaking,the convexity becomes an asymmetric peg and the concavity an asymmetric hole. The measured average tolerance for assembly (0.03 inches) is the same order of magnitude as camera projection factor. It is therefore necessary to tilt the piece in order to increase tolerances. After tilting tolerances are about the same as the concavity diameter. Geometry of the two puzzle pieces determines the actual tilting angle. Let us define a Cartesian Object System of Coordinates as presented in Fig. 4. Its origin is the center of gravity of the side with convexity (peg) P_1 , while Y_{obj} passes through G_1 . During tilting P_1 is maintained at fixed X,Y,Z robot coordinates. Robot target for tilting the piece thus becomes (8-11).

$$X_{tilt} = X_{rob} + \sin(\beta)(a - a\cos(\theta) + (b+f)\sin(\theta)) \quad (8)$$

$$Y_{tilt} = Y_{rob} - \cos(\beta)(a - a\cos(\theta) + (b+f)\sin(\theta)) \quad (9)$$

$$Z_{tilt} = Z_{rob} + (b+f)(\cos(\theta) - 1) + a\sin(\theta) \quad (10)$$

$$\text{Pitch} = \theta \quad (11)$$

$X_{rob}, Y_{rob}, Z_{rob}$ =robot coordinates
β = rotation angle between robot and object coordinate systems
a = distance from P_1 to G_1
b = handle length
f = distance from handle top to robot arm X,Y,Z link
θ= tilting angle

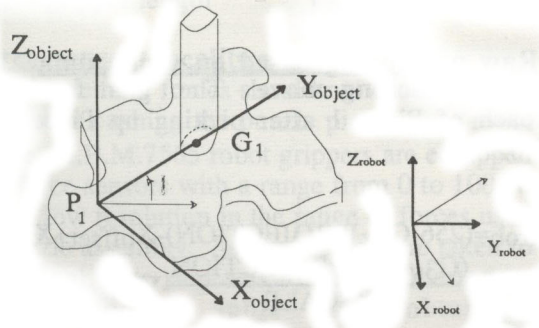

Fig. 4 Object system of coordinates

4.1.3 Bringing the pieces in contact This is the last move during raw positioning assembly. Here the free space assumption does not apply, since the move terminates upon contact with Piece 1. This is a different termination condition than for previous moves, and requires force feedback. Will and Grossman[11] call this type of moves *guarded moves*. Reaction forces are function of position errors that occur when the robot arm moves against obstacles as in (12).

$$F_r = \frac{x - x_c}{k} \quad (12)$$

F_r = sensed reaction force
x=robot actual position
x_c = robot commanded position
k = system stiffness constant

This termination condition applies to all transition and fine assembly moves used in our implementation.

4.2 Transition moves

These moves are done in order to nest the convexity on Piece 2 into the concavity of Piece 1. The first transition move is a sliding on top of Piece1 that terminates when contact is lost at edge 1, as presented in Fig. 5. Sliding is done along the generalized direction $P_1 G_1$. After edge 1 was detected, the next move is towards edge 2, where contact is reestablished. An average of the two termination points represents the target for next move. The same procedure is repeated for edge 3 and 4, but on a trajectory perpendicular to $P_1 G_1$. Averaging the four contact points eliminates translation errors induced by the vision system.

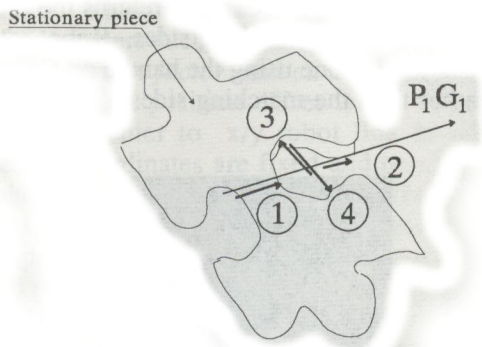

Fig. 5 Transition moves

4.3 Fine assembly moves

After completion of transition moves Piece 2 is nested with Piece 1, but on top of it and tilted as shown in Fig. 6. During fine assembly Piece 2 is pushed down into Piece 1 and then tilted back to a horizontal position.

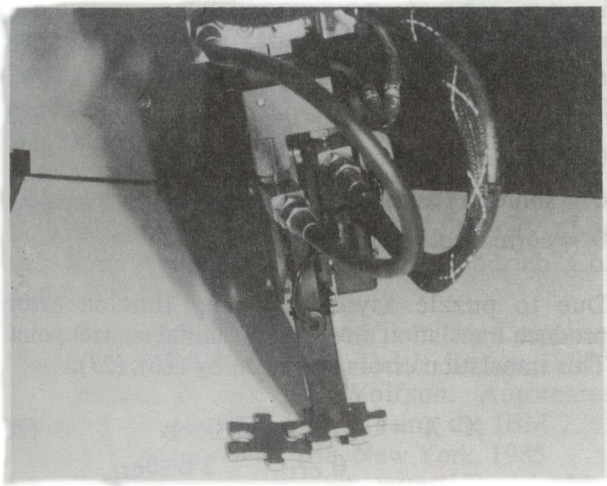

Fig. 6 Robot puzzle assembly

4.3 1. Push in move with rotation errors First the convexity of Piece 2 is brought in contact with Piece 1 by moving Piece 2 back to edge 1 along $G_1 P_1$. Once the contact established, the next move is a pushing of Piece 2 into Piece 1 with the target (13-16)

$$X_{pushin} = X_{rob} - t \sin(\beta)\sin(\theta) \quad (13)$$

$$Y_{pushin} = Y_{rob} + t \cos(\beta)\sin(\theta) \quad (14)$$

$$Z_{pushin} = Z_{rob} - t \cos(\theta) \quad (15)$$

$$Pitch = \theta \quad (16)$$

t= puzzle piece thickness

The tilting angle θ is such that if rotation errors exist the elbow of Piece 2 hits the top of Piece 1 before pushing in completes. The algorithm distinguishes between right or left elbow hit. In order to eliminate rotation errors, Piece 2 is rotated by an angle α, and the goal for this move is (17-20).

$$X_{rotation} = X_{rob} + (l \cos(\theta) - (f+b)\sin(\theta)) \quad (17)$$
$$(\sin(\alpha + \beta) + \sin(\beta))$$

$$Y_{rotation} = Y_{robot} + (l \cos(\theta) - (f+b)\sin(\theta)) \quad (18)$$
$$(\cos(\alpha + \beta) - \cos(\beta))$$

$$Z_{rotation} = Z_{rob} \quad (19)$$

$$Jaw_{rotation} = Jaw_{rob} + \alpha \quad (20)$$

α = rotation angle around contact point J

Rotation moves terminate when elbow contact between the two pieces is lost.

4.3.2Tilt back This last move brings Piece 2 to a horizontal position without loss of Piece 1. During this move the target is given by (21-24).

$$X_{tiltback} = X_{rob} + \sin(\beta + \alpha)(l - l\cos(\theta) - (f+b)\sin(\theta)) \quad (21)$$

$$Y_{tiltback} = Y_{rob} - \cos(\beta + \alpha)(l - l\cos(\theta) - (f+b)\sin(\theta)) \quad (22)$$

$$Z_{tiltback} = Z_{rob} + (f + b)(\cos(\theta) - 1) - l\sin(\theta) \quad (23)$$

$$Pitch_{tiltback} = Pitch_{rob} - \theta \quad (24)$$

5. Force history

Each gripper finger has tip, side and pitch strain gages giving 3D readings. Sensor readings are influenced by a number of factors such as orientation, sensor offset, calibration, mechanical amplification, crosstalk and vibrations. Previous experiments indicated that assembly force readings depend on gripper orientation during part pick up. It is therefore important to determine what is the best grasping position in order to maximize sensor output. We consider this to be a perpendicular to the general direction $P_1 G_1$, since this is the direction in which initial contact forces appear. Force readings during assembly are presented in Fig.7 and 8. These readings represent data that has been compensated for sensor offset and calibration. Measured force envelope during piece nesting is of the order of 5 N, which is slightly larger than anticipated. This may be due to the mechanical amplification effect of the handle-gripper combination. This force level meets conditions set in Section 2, which explains why no slip is present during initial assembly steps. Force readings are further influenced by cross coupling effects due to sensor design. Tests have shown that cross coupling accounts for about 5 to 10% residual force readings. Second order dynamic effects have not been considered here since assembly is done at very low speed (0.2 inch/second). Fig. 7 presents force data for nesting only, with no rotation error, while Fig. 8 shows forces during a complete assembly. During fine assembly forces occasionally pass the limit of magnetic pull resistance, and slip is present. When analyzing Fig. 18 we note a large tip force increase from A to B, followed by a sharp decrease C to D. These represent the end of raw positioning moves at point B and the detection of edge 1 at point D, as described in Section 4. Both sensor outputs follow the same pattern ABCDE, but separate

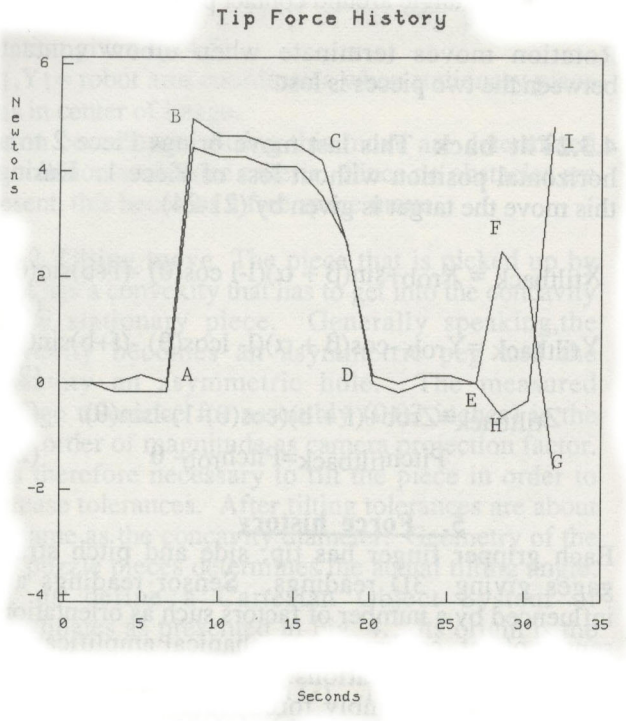

Fig. 7 Force history for raw and transition moves

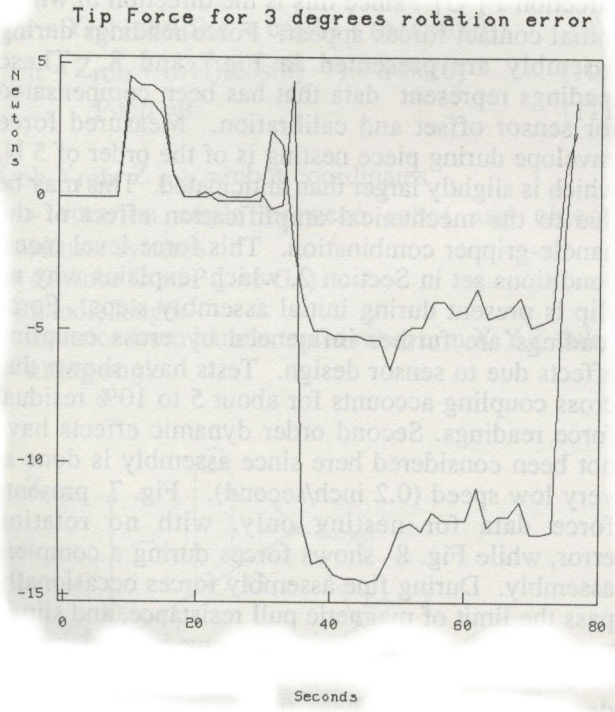

Fig. 8 Force history for complete assembly

along EFG and EHI respectively. This corresponds to nesting moves that detect edge 3 and 4. Here both sensors are subject to torques in opposing direction which explains the mirror symmetry of EFG versus EHI. The same general pattern is followed by side and pitch forces. It is important to estimate the limit on rotational and translational errors that an assembly algorithm can tolerate. The vision solution given as input to robot assembly algorithm may contain both rotation and translation errors. We define the vision rotation error θ_{err} as given by (25).

$$\theta_{err} = \theta' - \theta \tag{25}$$

θ_{err} =rotation error from vision solution

θ' = solution returned by vision match

θ = correct solution

Due to puzzle asymmetry, any rotation errors produce translation errors of the initial contact point. This translation errors are given by (26), (27).

$$X' - X = G_{3xrob'} - G_{3xrob} + 2(T+l)\sin\left(\frac{\theta_{err}}{2}\right)\cos\left(\frac{2\beta+\theta_{err}}{2}\right) \tag{26}$$

$$Y' - Y = G_{3yrob'} - G_{3yrob} + 2(T+l)\sin\left(\frac{\theta_{err}}{2}\right)\sin\left(\frac{2\beta+\theta_{err}}{2}\right) \tag{27}$$

X',Y' = robot coordinates of contact point with vision rotation error

X,Y = robot coordinates of contact point without rotation errors

θ_{err} = rotation error from vision given by (25)

$T = a - \cos(\theta)a + (b+f)\sin(\theta)$

Translation errors from vision may not be larger than the pseudo radius of the stationary puzzle concavity, or the peg will not intersect the concavity. The other condition requires the gripper to be as close as possible to the perpendicular to $P_1 G_1$, as discussed previously. An estimate for force sensor errors due to lack of proper positioning requires future work, while we presently address the geometrical condition only. For a pseudo radius of 0.25 inches, the condition set in (25) returns a maximum θ_{err} of 4 degrees for successful assembly. Tests have been run with rotation errors varying between 0 and 4.6 degrees. Successful nesting was obtained at initial rotation errors of 3 degrees, while the test failed at 4.6 degrees, results that confirm the theoretical prediction. Rotation error elimination had a success rate of about 50% mainly due to lack of force sensor sensitivity. In order to improve

assembly robustness it may be necessary to modify the nesting algorithm to take alternative actions in case edge 1 was not detected. The algorithm might reverse the scan on a perpendicular direction to $P_1 G_1$ to detect edge 3 and 4 and then detect edge 1 and 2.

Acknowledgement

Work on this project has been supported by Office of Naval Research Grant N00014-82-K-0381, National Science Foundation CER Grant DCR-83-20085, and by grants from the Digital Equipment Corporation and from I.B.M. Corporation.

References

1 BFgoodrich, Koroseal flexible Magnetic Sheet and Strip Application Guide, BFGoodrich Co., Akron, OH 1982.

2 Buckley S., Planning and Teaching Compliant Motion Strategies, MIT Ph. D. Thesis, Boston, 1987.

3 Burdea G. and H. Wolfson, Automated Assembly of a Jig-Saw Puzzle using the IBM 7565 Robot, NYUniversity TR 188, New York, 1985

4 Burdea G., Complex System and Tool for Fine Robot Assembly, NYUniversity, TR 276, 1986.

5 Inoue H., Force Feedback in Precise Assembly Tasks, MIT AIM-308, Boston, 1974.

6 Kalvin A.,E. Schonberg, J. Schwartz and M. Sharir, Two Dimensional Model Based Boundary Matching Using Footprints, NYUniversity TR 162, New York, 1985.

7 Lozano-Perez T., M. Mason and Taylor, Automated Synthesis of Fine-Motion Strategies for Robots, The International Journal of Robotics Research, Volume 3, MIT, 1984.

8 Lozano-Perez T., Automatic Planing of Manipulator Transfer Movements, Robot Motion, Planing and Control, pp 498-535, MIT, Press, 1985.

9 Seltzer D., Tactile Sensory Feedback for Difficult Robot Tasks, Robots6 Conference, SME TR MS82-220, 1982.

10 Simmunovich S., An Informational Approach to Parts Mating, MIT Ph. D. Thesis, Boston, 1979.

11 Will P. and D. Grossman, An Experimental System for Computer Controlled Mechanical Assembly, IEEE transactions on Computers, Volume 24, 1975.